Hindawi
Advances in Tribology
Volume 2024, Article ID 5541719, 11 pages
https://doi.org/10.1155/2024/5541719

Research Article

Mathematical Modeling of the Bearing Ratio Curve Rmr (50% Rz), through Investigation of the Effect of Process Parameters in Hard Turning of Steel C55 (DIN) with Mixed Ceramics MC2 ($Al_2O_3 + TiC$)

Mevludin Shabani [1] and Mite Tomov [2]

[1] *Faculty of Mechatronics, University for Business and Technology, Prishtina, Kosovo*
[2] *Faculty of Mechanical Engineering, Ss. Cyril and Methodius University, Skopje, North Macedonia*

Correspondence should be addressed to Mevludin Shabani; ludi62@yahoo.com

Received 8 September 2023; Revised 9 December 2023; Accepted 28 January 2024; Published 20 February 2024

Academic Editor: Mohammad Farooq Wani

The subject of modeling and predicting roughness parameters in hard machining has been discussed in many literature sources. However, most of these sources cover only the amplitude parameters such as Ra and Rz, leaving it unexplored to the right extent compared to its importance the roughness parameter bearing ratio curve (the Abbott–Firestone curve) which is essential in understanding the actual contact area of mating surfaces. To bridge this gap, this research has developed a mathematical model using the design of experiments method through investigation of the effect of process parameters in hard turning of Steel C55 (DIN) with mixed ceramics MC2 ($Al_2O_3 + TiC$). The model predicts the bearing ratio curve parameter Rmr (50% Rz), statistically processed using CADEX and Matlab. The research includes the ANOVA as a complementary tool in validating the generated mathematical model. The research analyzes the effects of material properties, cutting forces, and tool geometry as factors that affect the machining process. Additionally, it emphasizes the robustness of hard turning in consistently producing waviness patterns. Overall, this research provides valuable insights into the predictable effects of parameters on machined surfaces, which contributes to a better understanding of surface finish in metalworking.

1. Introduction

Generally, the production process faces many challenges, with market competition being the most significant. To succeed in this field, it is crucial to create strategies and guidelines that give you an edge over your competitors. Porter highlights that the competitive advantage comes from a range of unique activities that a company carries out in the different areas. These activities help to determine the company's cost position compared to its competitors and establish a foundation for differentiation [1].

Every task (activity) is aimed at producing high-quality products efficiently by utilizing crucial technological resources like raw materials, production technologies, skilled personnel, electricity, water, and transportation [2]. The manufacturing process ultimately affects the product's overall quality, which depends on its surface integrity. Surface integrity comprises several factors, including residual stress, hardness, phase transformation, microstructure, surface finish, and other topographical features [3]. The quality of a product is often determined by the roughness of its surface. This is also a crucial factor in adding value to the product. Measuring surface roughness is essential for achieving optimal machining performance, while also ensuring accurate dimensions. According to Rîpă et al. [4], specific engineering applications may require surfaces with particular topographical features that are beneficial for their intended use. In such cases, roughness parameters offer a comprehensive description of the surface topography [4]. The surface roughness quantity, reliability of cutting instruments, and product requirements are greatly influenced by machining

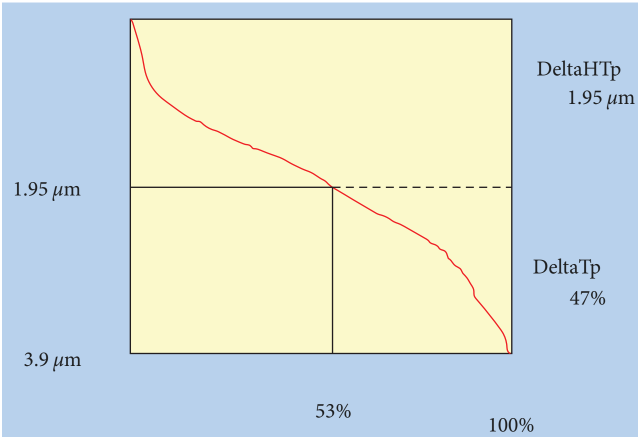

Figure 1: Material ratio curve (Authors).

parameters. When machining operations surpass the ideal technological values, it can lead to increased temperature and rate of chip formation [5]. Many attempts have been made to determine the ideal number of surface profile parameters that can predict the quality of a processed surface in terms of its roughness. However, the intricate nature of real surface geometry necessitates the consideration of numerous factors, methods, and measurement devices [6]. In the past, only a few amplitude parameters like Ra and Rz (Rt) were given importance in defining the machined surface roughness. But, these parameters alone cannot provide consistent results. Profiles with the same Ra and Rz values might differ in the shape of their asperities and spacing parameters. The latter plays a vital role in studying tribological phenomena [7]. Extensive research is crucial in evaluating numerous surface parameters that cannot fully explain surface texture. Roughness parameters Ra and Rz were thought to only indicate deviations from the average line in a vertical direction, without providing information about the shape, incline, or size of the asperities, or their frequencies. This can lead to differences in wear resistance, deformation upon contact, and peak wear volume for surfaces with the same Ra values but varying levels of wear resistance during the use. Ultimately, this discrepancy can affect the performance of machined surfaces [8].

When it comes to analyzing surfaces, there is a highly useful tool named the bearing ratio curve (Figure 1). It helps in understanding a surface's profile-bearing length ratio [9]. The tool works by examining the supporting span at different profile altitudes, which creates a clear bearing curve. This curve shows how much "solid" contact is left at any given point on the surface [6].

The ability to define profile roughness parameters is limited by the available methodologies and measurement techniques. To meet the growing demands for high-quality products, the development of advanced cutting materials, accurate measurement tools, and precise data processing software has become necessary. As a result of these advancements, sustainable product quality outcomes have been achieved. In the metalworking industry, grinding has traditionally been the final processing step. However, hard turning has gained popularity as a viable alternative with comparable results. Unlike grinding, hard turning has several advantages, such as a single setup, energy cost-effectiveness, and the absence of coolants, making it both economical and environmentally friendly. Numerous studies have highlighted the benefits of hard turning over grinding. According to Derakhshan and Akbari [10] hard turning can be a suitable substitute for conventional machining methods. As for Aslantas et al. [11], he suggests that hard turning is applicable for processing materials with a hardness level higher than 45 HRC, like steel. This method results in faster material removal, shorter setup times, and lower production costs [11]. When it comes to tribology, the way hard machining is completed is affected by a number of different factors such as cutting forces, tool wear, material properties, residual stresses, surface quality goals, and the temperature that develops between the tool and the work piece. Hard turning is a process that is used to achieve high-dimensional shape and surface accuracy during finishing or semifinishing. Materials used in hard turning can include heat-treated powder metallurgical parts, super alloys, irons, case-hardened steel, hard chrome-coated steel, hardened alloy steel, and tool steel [12]. When selecting materials that can withstand wear, it is important to consider their chemical composition properties. Studies so far suggest that the CBN tools provide superior results compared to grinding, and the micro-geometry of tool flank radii has a significant impact on machining performance. Extensive research recommends using CBN and ceramic tools for finishing hard materials due to their advantageous properties. This research involves experimental work using a ceramic cutting tool.

One of the most valuable methods in this field is statistical data processing of the experimental results. The Design of experiments (DoE) is a statistical/mathematical model that aids in planning experiments for data analysis using statistical methods, allowing for the derivation of valid and objective conclusions [13]. For this project, we utilized CADEX and Matlab. CADEX which stands for computer analysis and design of experiments was instrumental in assisting us with experimental design and statistical data processing [14]. In aim to increase the overall reliability of the research by providing a comprehensive and reliable assessment of the appropriateness of the mathematical model ANOVA is used as a complementary tool.

2. The Experimental Procedure

The experiment involved machining C 55 (DIN) steel rings with a specified hardness of 52 ± 2 HRC, specially designed for this purpose. The material C 55 (DIN) is medium carbon steel recognized for its suitability in high-strength applications, including automotive and general engineering components like axles, clutch members, shafts, pressed parts, piston rods, and gear racks [15]. The specimens used in this research had a diameter and length of Ø102 mm × Ø82 mm × 20 mm. During the machining process the rings were securely attached to a dedicated tool (Figure 2) to ensure precise positioning, stable cutting, and accurate measurement of surface layer roughness. An essential part of the experiment involved the thermal treatment of the steel rings. This treatment encompassed

Figure 2: Special setup for exploring characteristics of the surface layer during operation (Authors).

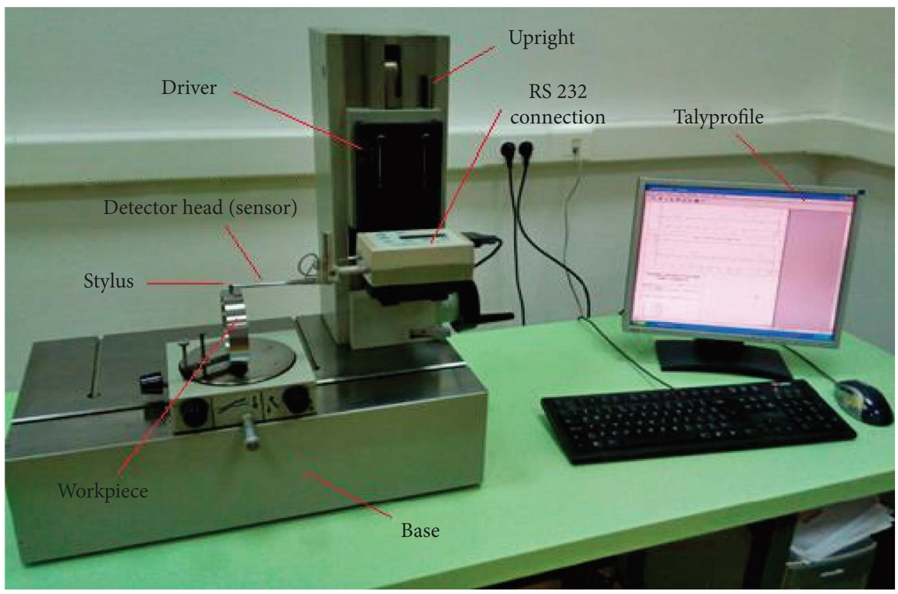

Figure 3: Surtronic 3+ gauging instrument and TalyProfile software (Authors).

preheating to 400°C for an hour, followed by heating to an austenitization temperature of 880°C for 50 min in an endothermic environment, with carbon potential adjustments based on the material's chemical composition. Tempering was carried out in a coolant with water additives to enhance the cooling rate, thereby increasing strength. The procedure was essential for eliminating residual stresses from prior treatments and achieving uniform structural conditions, resulting in the desired hardness of 52 ± 2 HRC. The careful approach to machining and thermal treatment ensured that the steel rings were prepared for subsequent testing and analysis, aligning with the specific objectives of the experiment and ensuring reliable results.

The turning process utilized a lathe with 11.2 kW power. Cutting employed SNGN 120708-120712-12-0716 inserts made of mixed ceramics MC2 (Al2O3) with specific tool geometry parameters. The choice of MC2 mixed ceramics, particularly Al2O3/TiC ceramics, stemmed from their ability to maintain physical–mechanical properties, high hardness, and wear resistance at elevated temperatures. In ceramic cutting, cutting speed significantly influences surface quality, with wear indicators assessing the cutting edge's state. Notably, mixed ceramics' significance in hard turning was emphasized by the various authors, showcasing its effectiveness in high-strength steel and ultra-high-strength steel turning. For example, Kumar et al. [16] evaluated the turning performance of Al2O3/TiC mixed ceramic cutting inserts with TiAlSiN coating in hard turning. Grzesik [17] also explored wear mechanisms in the turning of high-strength steel using $Al_2O_3 + TiC$ mixed ceramic tools. Wang et al. [18] on the other hand, investigated the fabrication and cutting performance of an Al2O3/TiC/TiN ceramic cutting tool in turning ultra-high-strength steel.

Table 1: Input variables.

No.	Factors	Code	1	0	−1
1	Speed (m/min)	X_1	130.00	94.00	64.00
2	Feed (mm/rot)	X_2	0.314	0.18	0.1
3	Depth cut (mm)	X_3	0.81	0.570	0.39
4	Tool radii (mm)	X_4	1.55	1.14	0.85

Each ring was subjected to three measurements and the average of the results was considered as the parameter value. The measuring device Surtronic 3+, as shown in the Figure 3, was employed to measure the roughness parameters and primary profiles of the machined surface. A Gaussian filter profile of

Table 2: Four factorial first-order design of the experiment.

Experiment No.	Encoded plan matrix					Rmr (50 Rz) (%)	Roughness Rz (μm)
	X_0	X_1	X_2	X_3	X_4		
1	1	−1	−1	−1	−1	—	—
2	1	1	−1	−1	−1	—	—
3	1	−1	1	−1	−1	—	—
4	1	1	1	−1	−1	—	—
5	1	−1	−1	1	−1	—	—
6	1	1	−1	1	−1	—	—
7	1	−1	1	1	−1	—	—
8	1	1	1	1	−1	—	—
9	1	−1	−1	−1	1	—	—
10	1	1	−1	−1	1	—	—
11	1	−1	1	−1	1	—	—
12	1	1	1	−1	1	—	—
13	1	−1	−1	1	1	—	—
14	1	1	−1	1	1	—	—
15	1	−1	1	1	1	—	—
16	1	1	1	1	1	—	—
17	0	0	0	0	0	—	—
18	0	0	0	0	0	—	—
19	0	0	0	0	0	—	—
20	0	0	0	0	0	—	—

Table 3: Four factorial first-order design of the experiment (real matrix).

Experiment No.	Input (process) parameters					Rmr (50 Rz) (%)	Roughness Rz (μm)
	X_0	v	f	a	r		
1	1	64.00	0.1	0.39	0.85	38.50	2.930
2	1	130.0	0.1	0.39	0.85	30.13	2.970
3	1	64.00	0.314	0.39	0.85	25.87	15.067
4	1	130.0	0.314	0.39	0.85	28.00	14.333
5	1	64.00	0.1	0.81	0.85	23.13	3.623
6	1	130.0	0.1	0.81	0.85	51.03	2.753
7	1	64.00	0.314	0.81	0.85	29.03	15.500
8	1	130.0	0.314	0.81	0.85	28.23	14.400
9	1	64.00	0.1	0.39	1.55	33.50	2.073
10	1	130.0	0.1	0.39	1.55	53.20	1.443
11	1	64.00	0.314	0.39	1.55	36.37	7.093
12	1	130.0	0.314	0.39	1.55	40.10	6.393
13	1	64.00	0.1	0.81	1.55	39.17	1.767
14	1	130.0	0.1	0.81	1.55	44.93	1.870
15	1	64.00	0.314	0.81	1.55	30.10	7.720
16	1	130.0	0.314	0.81	1.55	3433	8.360
17	0	94.00	0.180	0.570	1.14	25.97	5.290
18	0	94.00	0.180	0.570	1.14	23.95	5.590
19	0	94.00	0.180	0.570	1.14	24.30	5.280
20	0	94.00	0.180	0.570	1.14	19.93	4.587

0.8 mm was used to separate the roughness profiles from the primary profile. During the measurement process, an elementary measuring length of 0.8 mm and a total measuring length of 4 mm were adopted. The TalyProfile software was utilized for calculating the roughness parameters of the profile measurement.

3. Results

When determining the bearing ratio curve through experimentation, there are several critical geometric factors to consider. The cutting speed, cutting feed, cutting depth,

Table 4: Correlation of the input–output information about the mathematical model.

A first-order mathematical model without interaction or assessment of the significance of the factors				
Number of experiments	Calculated values Rmr (%)	Predicted values Rmr (%)	Error (%)	95% Confidence interval
1	38.500	29.183	24.201	21.956–38.787
2	30.130	34.878	−15.757	26.241–46.357
3	25.870	23.987	7.281	18.047–31.881
4	28.000	28.667	−2.384	21.569–38.103
5	23.130	28.404	−22.802	21.370–37.752
6	51.030	33.947	33.476	25.541–45.120
7	29.030	23.346	19.578	17.565–31.030
8	28.230	27.902	1.160	20.993–37.086
9	33.500	36.366	−8.557	27.361–48.336
10	53.200	43.463	18.302	32.701–57.768
11	36.370	29.891	17.814	22.489–39.729
12	40.100	35.724	10.912	26.878–47.482
13	39.170	35.396	9.635	26.631–47.046
14	44.930	42.303	5.846	31.828–56.227
15	30.100	29.094	3.344	21.889–38.669
16	34.330	34.771	−1.285	26.161–46.215
17	25.970	31.855	−22.659	28.361–35.778
18	23.950	31.855	−33.004	28.361–35.778
19	24.300	31.855	−31.089	21.956–35.778
20	19.930	31.855	−59.832	26.241–35.000

Table 5: Assessment of the significance of factors.

Mathematical model of the first order without interaction of factors							
	Coefficients of the mathematical model						
Index	Coded	Decoded	Degree of freedom	Sum of squares (SS)	Dispersion S/F	Dispersion ratio FR	Assessment of the significance
0	3.461	6.384	1	239.596	239.596	18,630	Significant
1	0.08913	0.2599983	1	0.127120	0.127120	9.9	Insignificant
2	−0.09804	−0.1708942	1	0.153796	0.153796	12.0	Significant
3	−0.01352	−0.0390300	1	0.002926	0.002926	0.22753	Insignificant
4	0.11003	0.3174936	1	0.193723	0.193723	15.1	Significant
	FR < 10,130 ≥ insignificant				FR > 10,130 ≥ insignificant		

Table 6: Summary output.

Regression statistics	
Multiple R	0.949578716
R square	0.901699738
Adjusted R square	0.875486335
Standard error	1.696508513
Observations	20

and tool nose radius all have significant tribological implications that affect the frictional forces, heat generation, and wear rates experienced at the tool-workpiece interface. To achieve a stable machining process, it is essential to optimize these factors. Cutting speed affects temperature and friction, while cutting depth and feed impact contact pressures and wear. The tool nose radius produces stress distribution. Properly managing these geometric factors ensures stability by minimizing wear and heat buildup, while maintaining efficient material removal. By doing so, a reliable and controlled machining operation is achieved. The radius of the cutting tool has been researched in this case as a tendency to multiply the factors that influence the machining process, so we consider that it represents a novelty in this context because most of the research so far in this field considers only parameters, such as cutting speed, feed, and depth, so, the radius is combined as an additional parameter, to obtain more complete results in gaining much more information on processed material, tool cutting material, and the process itself.

The research employs the various activities, highlighting the importance of systematic planning, data collection, and model development. It underscores the iterative nature of the research process, where adjustments are made based on the

Table 7: ANOVA analysis.

ANOVA						
	df	SS	MS	F	Significance F	
Regression	4	396.0140679	99.003517	34.3984233	2.1586E-07	
Residual	15	43.17211701	2.87814113	—	—	
Total	19	439.186185	—	—	—	
	Coefficients	Standard error	t Stat	P-value	Lower 95%	Upper 95%
Intercept	5.272819	2.393102	2.203341	0.043617	0.172044	10.373594
v	−0.004512	0.012094	−0.373094	0.714299	−0.030290	0.021265
f	41.208077	3.914468	10.527120	0.000000	32.864585	49.551569
a	1.398816	2.114688	0.661477	0.518339	−3.108534	5.906167
r	−6.299031	1.208336	−5.212982	0.000105	−8.874538	−3.723525

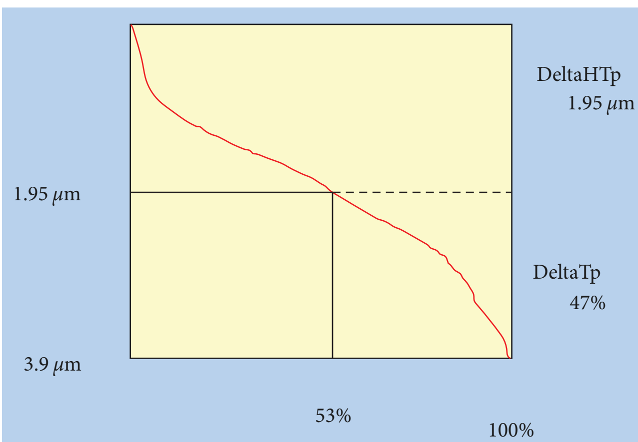

Figure 4: Material ratio curve for roughness profile, experiment 1-1 at $v = 67$ (m/min); $f = 0.1$ (mm/rot).

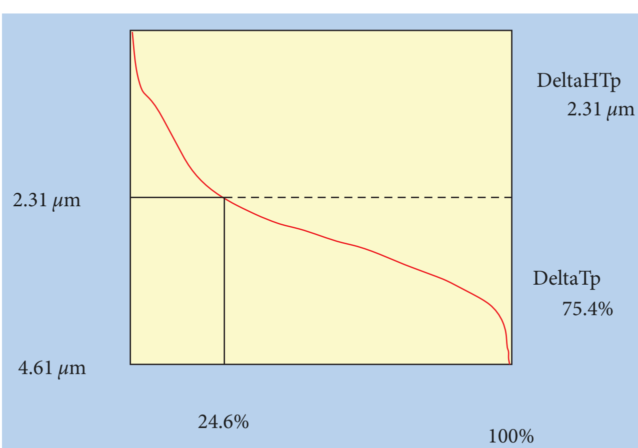

Figure 5: Material ratio curve for roughness profile, experiment 5-1 at $v = 67$ (m/min); $f = 0.1$ (mm/rot).

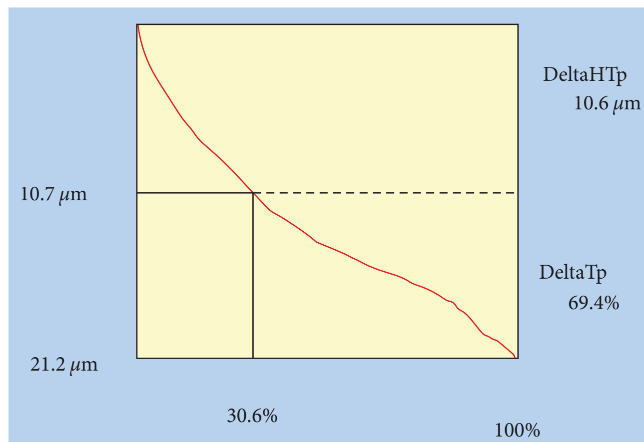

Figure 6: Material ratio curve for roughness profile, experiment 7-1 at $v = 67$ (m/min); $f = 0.315$ (mm/rot); $a = 0.8$ (mm); and $r = 0.8$ (mm).

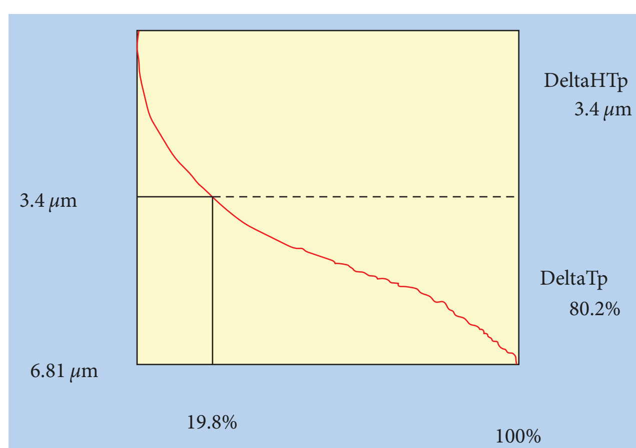

Figure 7: Material ratio curve for roughness profile, experiment 20-1 at $v = 94$ (m/min); $f = 0.18$ (mm/rot); $a = 0.56$ (mm); and $r = 1.2$ (mm).

accuracy of the mathematical model. The initial step in experimental research, involves finding a mathematical model to describe measured values accurately. This concept aligns with the work of Box and Draper [19] who emphasized the importance of designing experiments to fit mathematical models, underscoring that the choice of experimental design directly affects the accuracy of the model. The next step involves selection of appropriate measurement units and techniques. This phase is crucial for obtaining reliable data. In his book on

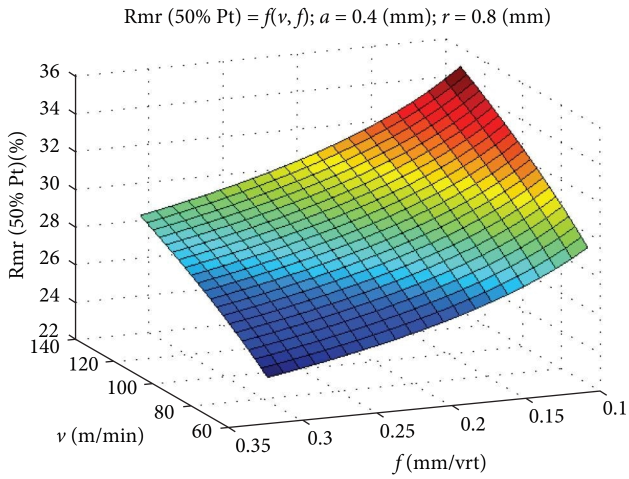

Figure 8: Graphic representation of roughness parameter Rmr (50% Rz) as a function of cutting speed v (m/min) and feed f (mm/rot) for $a = 0.4$ (mm) and $r = 0.8$ (mm).

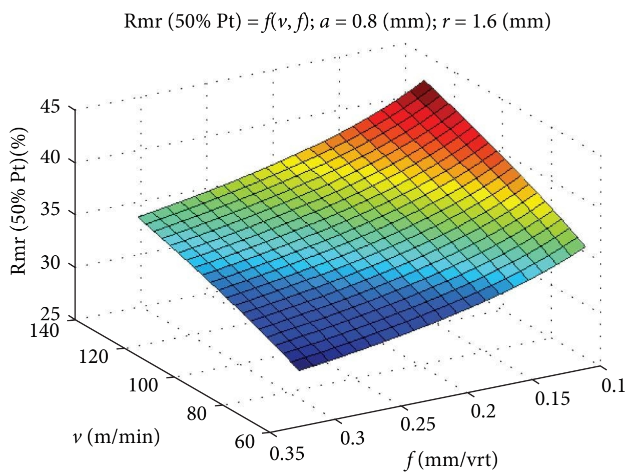

Figure 9: Rmr (50% Rz) as a function of cutting speed v (m/min) and feed f (mm/rot), at $a = 0.8$ (mm) and $r = 1.6$ (mm).

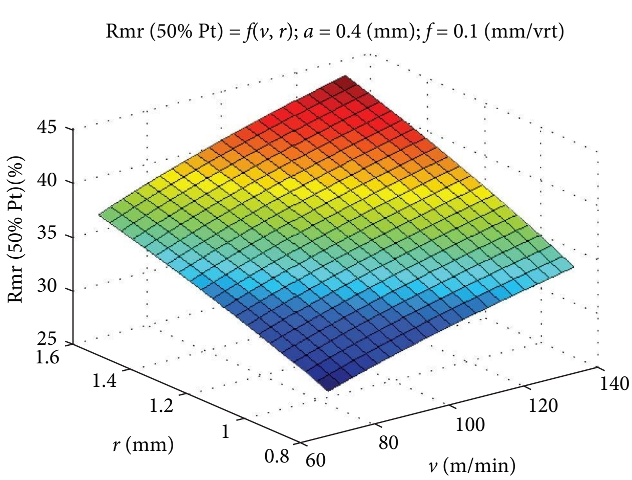

Figure 10: Graphic representation of roughness parameter Rmr (50% Rz) as a function of cutting speed v (m/min) and nose radius r (mm), at $a = 0.4$ (mm) and $f = 0.1$ (mm/rot).

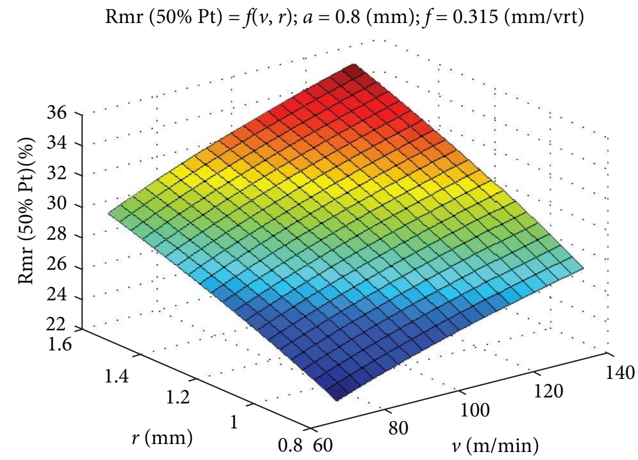

Figure 11: Graphic representation of Rmr (50% Rz) vs. cutting speed v (m/min) and cutting insert nose radius r (mm) at $a = 0.8$ (mm) and $f = 0.315$ (mm/rot).

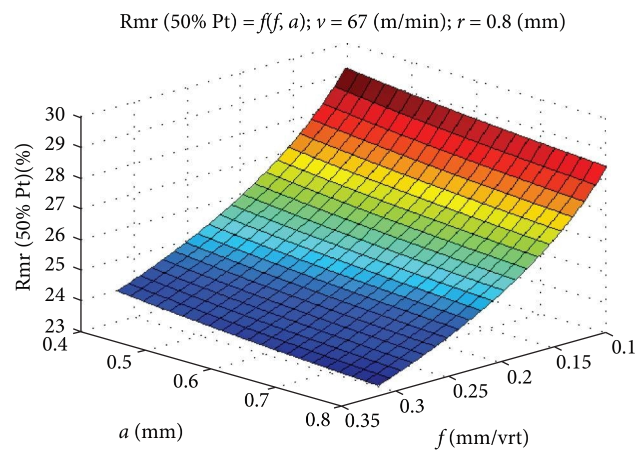

Figure 12: Graphic display of Rmr (50% Rz) as a function of f (mm/rot) and a (mm) at $v = 67$ (m/min) and r = 0.8 (mm).

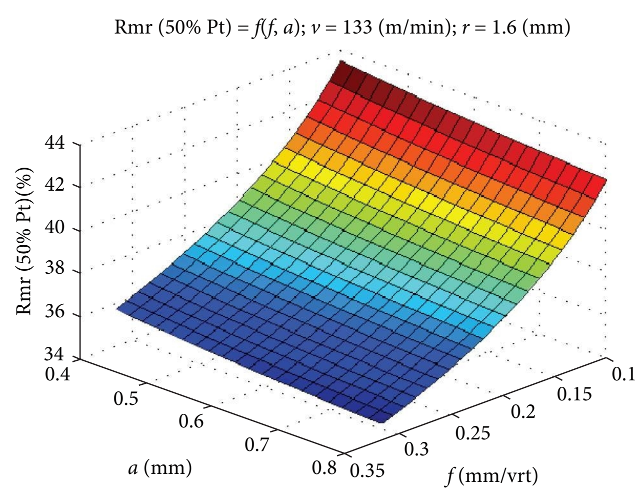

Figure 13: Graphic display of the roughness parameter Rmr (50% Rz) as a function of the feed f (mm/feed) and the depth of cut a (mm), at $v = 133$ (m/min) and $r = 1.6$ (mm).

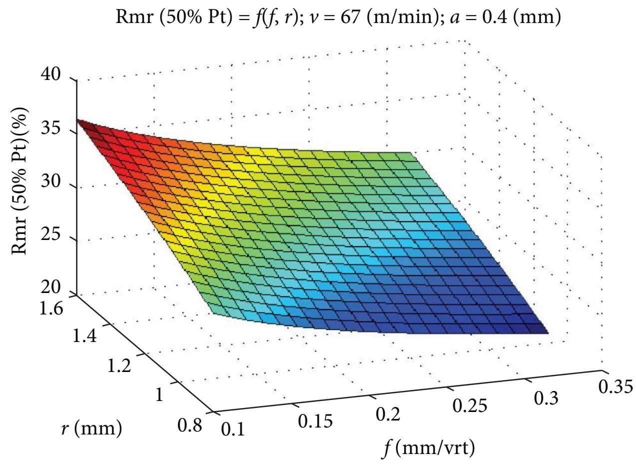

FIGURE 14: Graphic representation of the roughness parameter Rmr (50% Rz) as a function of the feed f (mm/rot) and the cutting nose insert radius r (mm), at $v = 67$ (m/min) and $a = 0.4$ (mm).

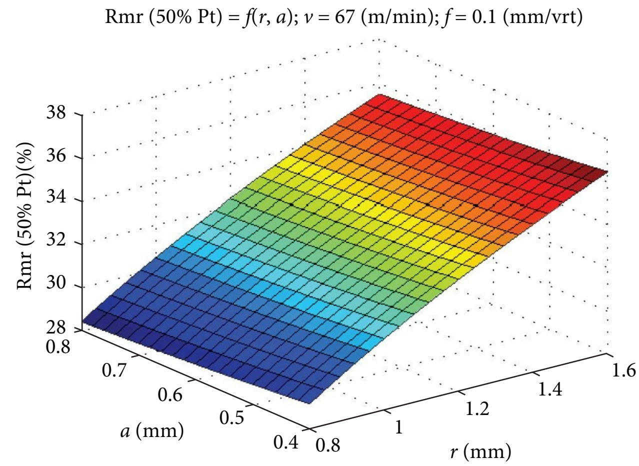

FIGURE 16: Graphic representation of the roughness parameter Rmr (50% Rz) (%) as a function of the cutting insert radius r (mm) and the depth of cut a (mm), at $v = 67$ (m/min) and $f = 0.1$ (mm/rot).

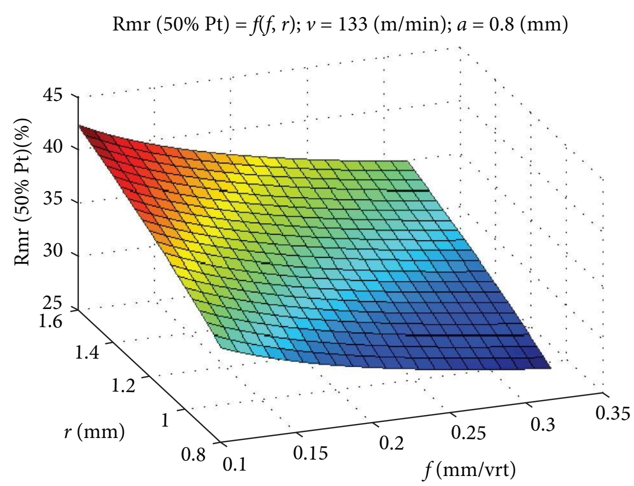

FIGURE 15: Graphic representation of the roughness parameter Rmr (50% Rz) % as a function of the feed f (mm/rot) and the radius of the tip of the cutting nose insert radius r (mm), at $v = 133$ (m/min).

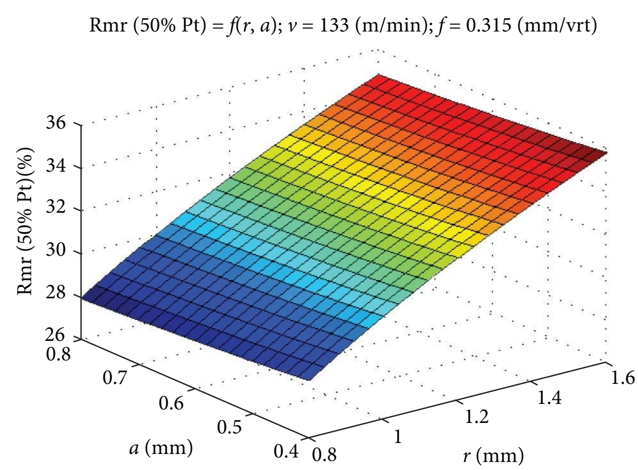

FIGURE 17: Graphic representation of the roughness parameter Rmr (50% Rz) (%) as a function of the cutting insert radius r (mm) and the cutting depth a (mm), at $v = 133$ (m/min) and $f = 0.315$ (mm/rot).

experimental design, Montgomery [13] highlights the significance of careful planning and measurement selection to minimize errors and bias in data collection. Furthermore, the study emphasizes the iterative nature of experimental research, where adjustments may be needed if the accuracy of the model is insufficient. This iterative approach resonates with the principles of the Plan-Do-Study-Act (PDSA) cycle, commonly used in quality improvement and research. The PDSA cycle emphasizes continuous improvement through iterative cycles of planning, implementation, observation, and adjustment [20].

The activities described above align with established principles in experimental research and quality improvement. Careful planning, measurement selection, and iterative refinement are essential for obtaining accurate mathematical models that describe real-world phenomena. A power shape function is adopted to describe the subsequent changes in roughness. To determine unknown values (C, x, y, z, and q) in a mathematical model Equation (1), a systematic approach is employed, which involves several key steps and statistical techniques.

$$\text{Rmr}\,(50\%\,\text{Rz}) = C \cdot v^{x} \cdot f^{y} \cdot a^{z} \cdot r^{q}. \quad (1)$$

Table 1 displays the machining variations for process factors in accordance with the aforementioned steps.

A carefully planned set of experiments, totaling $2^4 + 4$, is executed. The results from these experiments, recorded in Tables 2 and 3, provide the data necessary for further analysis.

A research was carried out to investigate the relationship between the input and output data. The predictions were found to be satisfactory and the model's accuracy was confirmed with a 95% confidence interval (these intervals establish the range in which the true coefficients are likely to fall, providing precision estimates). The deviations between the calculated and predicted Rmr (50% Rz) values are presented in Table 4, in which deviations range from 33% for experiment Nr. 6 to −59.832% for experiment Nr. 20 were observed for Rmr (50% Rz). In the statistical analysis, we chose the mode that does not involve interaction or significance of factors. This confirms that the model is appropriate for representing physical and technological effects during cutting processes, impacting machined surfaces. The accuracy of the function that explains the phenomena being researched was not affected, even though independent variables (v, f, a, and$r$) were kept separate. The correlation between the input and output information of the mathematical model is presented in Table 4.

To assess the significance of factors (Table 5) in the regression polynomial, the Fisher test is employed at a significance level (α) of 0.05. This test helps identify which variables have a statistically significant impact on the dependent variable, aiding in model refinement.

The selection of the mathematical model is settled based on the analysis of the characteristics of the given model, including details such as the number of terms in the regression polynomial, residual sum, adequacy coefficient, experimental error, and the multiple regression coefficients.

Based on the experimental data obtained, and statistical processing, the following mathematical model (Equation (2)) for the roughness parameter Rmr (50% Rz) is generated:

$$\mathrm{Rmr}\,(50\%\,\mathrm{Rz}) = 6.834 \cdot v^{0.2599983} \cdot f^{-0.1708942} \cdot a^{-0.0390200} \cdot r^{0.317493}. \tag{2}$$

In conclusion, this systematic methodology ensures a data-driven approach to determine unknown coefficients, emphasizing efficiency in extracting valuable information from a minimal number of experiments.

To support our approach about the accuracy of our model, the results of experiments in Tables 2 and 3 were then analyzed by using ANOVA statistical package (Tables 6 and 7). ANOVA helped in assessing the significance of experimental variations and complements the precision of the mathematical model. This approach provides a complete assessment, confirming the alignment with the data validity identified by the CADEX software.

After performing the required calculations, we have come to the conclusion that the ANOVA outcomes are quite analogous to the results obtained with CADEX (viewed from the aspect of the validity of the results from each method independently), with some insignificant variances that can be credited to technological advancements; this is expected and understandable. Despite the differences mentioned above, it can be concluded that the model's adequacy is not in question.

Upon analyzing the mathematical expression Equation (2), which takes into account the impact of all technological factors, it becomes clear that the value of every process parameter depends on its respective exponent. A positive exponent results in an increase in roughness, while a negative exponent decreases it.

Parallelly graphical results, unambiguously explain considered surfaces where variations in the bearing curve can be observed. Observing alternations of the process parameter values, affecting the shape of the bearing ratio curve, certainly can be concluded about the different wear resistance of surfaces, the way of the contact formation, the wear of the profile peaks, etc. The findings indicate not only the change in the character of the bearing curve but also the difference in the coefficient of the bearing length of the profile, depending on Rz depth (in our case 0.5).

An analysis of the mathematical model Equation (2), as well as a graphical presentation of the bearing curve of the profile (out of a total of 60×3 experimental measurements) Figures 4–7 will be presented, which best express the change in the bearing curve, making it possible to formulate that the obtained mathematical model, based on the results of the experimental work allows conclusions and observations.

To visually compare the experimental data with the model output, contour plots are used (Figures 8–17).

4. Conclusion

To put it simply, the assessment of the hard-turning method hinges on closely examining key factors, particularly the numbers used as exponents in the math equation. This mathematical framework is the foundation for how well the experimental model fits. When these two parts come together, we get a complete view that aims to prove how effective the hard-turning technique really is.

But getting a clear evaluation is not easy. Things like vibrations or unexpected obstacles can mess up the results. This might mean the roughness pattern does not show up the same way, making it hard to tell if the model is good enough. This is where the reliability of the model and the stability of the cutting process meet and interact. On the other side, when the cutting process stays stable, we see a consistent roughness pattern. This reliability shows that the mathematical model and the real-world testing agree with each other. The careful balance between theory and actual testing gives the whole process more credibility. Notably, the mathematical model keeps being tested throughout the experiments, making the conclusions even stronger.

Understanding the alterations that occur when we adjust various elements of the procedure is a significant aspect of this. Among all these changes, the waviness pattern remains quite steady. This consistency is interesting, even though the process changes, the basic waviness traits, like size and shape, remain quite steady. This robustness is a key feature of the hard-turning method.

These patterns result from variations in the roughness parameter Rmr (50% Rz) based on different process parameters, including cutting speed v, cutting feed rate f, depth of the cut a, and cutting nose radius r. The research suggests that each parameter has a specific and consistent impact on the roughness or waviness of the machined surface. Let us examine the effects of each process parameter in more detail: Increasing the cutting speed v causes a proportional change in the linear bearing of the roughness profile at a depth of 0.5 Rz. This means that as the cutting speed increases, the waviness pattern in the roughness profile changes consistently and proportionally at this specific depth. The cutting feed rate f has a significant and dual influence on the coefficient of the bearing length of the profile; at a depth of 0.5 Rz, it shows an inversely proportional effect while at lower depths (Rz), it tends to get proportional. This implies that the waviness pattern changes differently at different depths depending on the feed rate. The cutting depth a shows an inversely proportional effect on the bearing length coefficient of the profile. The effect is small and becomes even smaller with increasing depth. In other words, the waviness pattern changes consistently, but it is more pronounced at shallower depths. The cutting tool nose radius r has a directly proportional effect on the profile of the bearing curve. This means that as the cutting nose radius increases, the waviness pattern in the roughness profile changes consistently and proportionally.

To summarize, the research suggests that these process parameters have predictable and consistent effects on the waviness patterns of the roughness profile. These patterns indicate the strength of the method in controlling and understanding the effects of these parameters on the surface finish of machined parts. Furthermore, the study notes that an increase in wear of the cutting insert leads to specific changes in the roughness profile, including an increase in height and amplitude parameters, a decrease in horizontal parameters, and a change in the bearing length coefficient of the roughness profile Rmr (50% Rz).

The results of all this testing have real technical significance. What we learn from matching math and real-world results could reshape how we work with metal. By fine-tuning processes based on the tested math, we could make big improvements. These improvements in the larger industrial picture could lead to real economic gains.

So, in a nutshell, evaluating the hard-turning method is not straightforward. It is a mix of careful math and practical tests that validate each other. In the face of challenges and stability, the consistent waviness patterns show the method's strength. This is not just about theory—it has the power to change how industries work and bring in actual economic benefits.

Data Availability

The data used to support the findings of this study have been deposited in the University "Goce Delchev" in Shtip (North Macedonia) repository. The research work has been developed at the Laboratory for Production Technologies and Processes, and the Laboratory for Metrology and Geometric Characteristics and Quality Control at the "Ss. Cyril and Methodius" University in Skopje, Faculty of Mechanical Engineering—Skopje, North Macedonia,

Conflicts of Interest

The authors declare that they have no conflicts of interest.

Acknowledgments

I am grateful to Professor Mite Tomov for his valuable support during our research project. I also want to express my appreciation to Professor Mikolaj Kuziovski (in memoriam) for providing the necessary resources and equipment to carry out the experimental research conducted at the Faculty of Mechanical Engineering in Skopje. The reimbursement for the research is expected to be made by the Ministry of Education in Kosovo through funds dedicated for this purpose, however, the reimbursement does not cover the expenses. This reimbursement is made after the eventual publication of the work.

References

[1] M. E. Porter, *Competitive Advantage: Creating and Sustaining Superior Performance*, pp. 73–93, Free Press, New York, 1995.

[2] M. Kuzinovski, *Investigation of phisical phenomena and technological effects in turning with increased cutting speeds*, Ph D thesis, Faculty of Mechanical Engineering, Skopje, 1991.

[3] D. Ulutan and T. Ozel, "Machining induced surface integrity in titanium and nickel alloys: a review," *International Journal of Machine Tools and Manufacture*, vol. 51, no. 3, pp. 250–280, 2011.

[4] M. Rîpă, L. Tomescu, M. Hapenciuc, and I. Crudu, "Tribological characterisation of surface topography using Abbott–Firestone curve," in *National Tribology Conference*, pp. 208–212, University "Dunărea de Jos" of Galati, Români, 2003.

[5] M. Tomov, M. Kuzinovski, and P. Cichosz, "Development of mathematical models for surface roughness parameter prediction in turning depending on the process condition," *International Journal of Mechanical Sciences*, vol. 113, pp. 120–132, 2016.

[6] E. S. Gadelmawla, M. M. Koura, T. M. A. Maksoud, I. M. Elewa, and H. H. Soliman, "Roughness parameters," *Journal of Materials Processing Technology*, vol. 123, no. 1, pp. 133–145, 2002.

[7] I. V. Kragel'skii, M. N. Dobychin, and V. S. Kombalov, *Fundamentals of Calculations for Friction and Wear*, Elsevier Science, 1977.

[8] W. P. Dong, P. J. Sullivan, and K. J. Stout, "Comprehensive study of parameters for characterising three-dimensional surface topography: III: Parameters for characterising amplitude and some functional properties," *Wear*, vol. 178, no. 1-2, pp. 29–43, 1994.

[9] Michigan Metrology, L. L. C., "3D surface roughness and wear measurement, analysis and inspection," 2022, https://michmet.com/surface-roughness-analysis-blog-stylus-xy-parameters.

[10] E. D. Derakhshan and A. A. Akbari, "Experimental investigation on the effect of workpiece hardness and cutting speed on surface roughness in hard turning with CBN tools," in *Proceedings of the World Congress on Engineering*, vol. 2, pp. 1–3, 2009.

[11] K. Aslantas, I. Ucun, and A. Cicek, "Tool life and wear mechanism of coated and uncoated Al_2O_3/TiCN mixed ceramic tools in turning hardened alloy steel," *Wear*, vol. 274, pp. 442–451, 2012.

[12] GEAR Solutions and C. Richt, "A hard turn toward efficiency," 2009, https://gearsolutions.com/features/a-hard-turn-toward-efficiency/.

[13] D. C. Montgomery, *Design and Analysis of Experiments*, John Wiley & Sons, 2017.

[14] N. Trajchevski, M. Kuzinovski, and P. Cichosz, "Investigation of temperature during machining process by high speed turning," 2009.

[15] Holden Special Steel, "C55 Carbon steel |DIN1.0535 | AISI 1055| S55C," 2023, https://www.round-bars.com/products/c55-steel/.

[16] C. S. Kumar, S. K. Patel, and F. Fernandes, "Performance of Al2O3/TiC mixed ceramic inserts coated with TiAlSiN, WC/C and DLC thin solid films during hard turning of AISI 52100 steel," *Journal of Materials Research and Technology*, vol. 19, pp. 3380–3393, 2022.

[17] W. Grzesik, "Wear development on wiper Al2O3-TiC mixed ceramic tools in hard machining of high strength steel," *Wear*, vol. 266, no. 9-10, pp. 1021–1028, 2009.

[18] D. Wang, C. Xue, Y. Cao, and J. Zhao, "Fabrication and cutting performance of an Al_2O_3/TiC/TiN ceramic cutting tool in turning of an ultra-high-strength steel," *The International Journal of Advanced Manufacturing Technology*, vol. 91, no. 5–8, pp. 1967–1976, 2017.

[19] G. E. Box and N. R. Draper, *Empirical Model-Building and Response Surfaces*, John Wiley & Sons, 1987.

[20] G. J. Langley, R. D. Moen, K. M. Nolan, T. W. Nolan, C. L. Norman, and L. P. Provost, *The Improvement Guide: A Practical Approach to Enhancing Organizational Performance*, John Wiley & Sons, 2009.